P7.3 AN ENHANCED GLOBAL PRECIPITATION MEASUREMENT (GPM) VALIDATION NETWORK PROTOTYPE

AN ENHANCED GLOBAL PRECIPITATION MEASUREMENT (GPM) VALIDATION NETWORK PROTOTYPE

K. Robert Morris*
SAIC / NASA / Goddard Space Flight Center
Mathew R. Schwaller – NASA/GSFC

1. INTRODUCTION

A Validation Network (VN) prototype is currently underway that compares data from the Tropical Rainfall Measuring Mission (TRMM) satellite Precipitation Radar (PR) to similar measurements from U.S. and international operational weather radars. This prototype is a major component of the Ground Validation System (GVS) activities supporting the Global Precipitation Measurement (GPM) mission. The purpose of the VN is to provide a means for the precipitation community to identify and resolve significant discrepancies between the ground radar (GR) observations and satellite observations. The ultimate goal of such comparisons is to understand and resolve the first order variability and bias of precipitation retrievals in different synoptic regimes at large scales. The VN prototype is based on research results and computer code described by Anagnostou et al. (2001), Bolen and Chandrasekar (2000), and Liao et al. (2001), and has previously been described by Morris, et al. (2007). This paper describes a major algorithmic improvement to the PR-to-GR volume matching procedures, new tools for analysis of the volume matched data, and updated statistical results for PR-GR reflectivity comparisons.

2. VN DATA COLLECTION AND PROCESSING

The core VN dataset consists of matched TRMM PR and quality-controlled, ground-based WSR-88D (Weather Surveillance Radar – 1988 Doppler, or WSR-88D) radar reflectivity, for 21 sites in the Southeastern U.S. located within a bounding rectangle extending from 24° to 35° N latitude and 80° to 98° W longitude (Table 1). The current period of record for the VN data for the core sites starts on August 8, 2006 and runs to the present. Other ground radar sites that have contributed data to the VN for selected dates include the Gosan, South Korea S-band radar of the National Institute of Meteorological Research (METRI) of the Korea Meteorological Administration (KMA), the Advanced Radar for Meteorological and Operational Research (ARMOR) dual-polarimetric C-band Doppler radar, the Australian Bureau of Meteorology (BOM) (DARW) CPOL radar (Keenan et al., 1998), and Kwajalein dual-polarization S-band Doppler radar (Schumacher and Houze, 2000, and Wolff et al., 2005).

The data ingest and preprocessing component of the VN software ingests and stores TRMM PR and coincident ground radar data whenever an "overpass event" occurs. Such an event takes place any time the TRMM PR ground track passes within 200 km of a VN ground radar (GR) site. For each overpass event, the GR volume scan beginning at or just prior to the satellite overpass time is acquired along with its corresponding PR data. GR data for the WSR-88D sites are acquired and quality controlled on a routine, operational basis by the VN, via the TRMM Ground Validation Office. Data for other the ground radar sites are currently acquired by the VN on an ad-hoc basis from the data providers.

Site ID	Site name	Latitude deg. N	Longitude deg. E
KAMX	Miami, FL	25.6111	-80.4128
KBMX	Birmingham, AL	33.1722	-86.7697
KBRO	Brownsville, TX	25.9161	-97.4189
KBYX	Key West, FL	24.5975	-81.7031
KCLX	Charleston, SC	32.6556	-81.0422
KCRP	Corpus Christi, TX	27.7842	-97.5111
KDGX	Jackson, MS	32.3178	-89.9842
KEVX	Eglin AFB, FL	30.5644	-85.9214
KFWS	Dallas-Ft Worth, TX	32.5731	-97.3031
KGRK	Fort Hood, TX	30.7219	-97.3831
KHGX	Houston, TX	29.4719	-95.0792
KHTX	Huntsville, AL	34.9306	-86.0833
KJAX	Jacksonville, FL	30.4847	-81.7019
KJGX	Robins AFB, GA	32.6753	-83.3511
KLCH	Lake Charles, LA	30.1253	-93.2158
KLIX	Slidell, LA	30.3367	-89.8256
KMLB	Melbourne, Florida	28.1133	-80.6542
KMOB	Mobile, AL	30.6794	-88.2397
KSHV	Shreveport, LA	32.4508	-93.8414
KTBW	Tampa Bay, FL	27.7056	-82.4017
KTLH	Tallahassee, FL	30.3975	-84.3289
RGSN	*Gosan, Korea*	*33.2942*	*126.1630*
RMOR	*ARMOR/Huntsville*	*34.6460*	*-86.7700*
DARW	*Darwin*	*-12.2522*	*131.0430*
KWAJ	*Kwajalein atoll*	*8.7180*	*167.7330*

Table 1. Ground radar sites included in the current GPM GVS Validation Network prototype. Except those in italics, all are WSR-88D radars.

PR data are extracted from standard TRMM Version 6 data products 1C-21, 2A-23, 2A-25, and 2B-31 for orbital overpass events where the instrument ground track coincides with a VN ground radar. The extracted PR data include radar reflectivity (both raw and attenuation corrected), near-surface rain rate, and other

*Corresponding author address: K. Robert Morris, NASA/GSFC Code 422, Greenbelt MD 20771.
E-mail: Kenneth.R.Morris@nasa.gov

variables. The VN acquires PR data as orbit subset products, for single radars or adjacent groups of radars, directly from NASA's Precipitation Processing System (PPS, http://pps.gsfc.nasa.gov/pps). The PR data, along with detailed product descriptions, are also available to the public via NASA's Goddard Earth Sciences Data and Information Services Center (GES DISC, http://disc.sci.gsfc.nasa.gov). All data acquired by the VN are stored permanently in the VN file system, unmodified and in their native format.

Selected fields of the PR products are analyzed upon receipt to temporary 75-by-75 point Cartesian grids of 4-km resolution, one centered on each ground radar site overpassed by the TRMM satellite in the given orbit. The VN software harvests metadata parameters for each site overpass event from the temporary grids. These parameters characterize the precipitation and radar echo characteristics of the event. The metadata are stored in the VN relational database and are linked through the database to the associated PR orbit subset and GR data files. Metadata parameters stored include the average height of the bright band over the analysis area, and the number of grid points:

- in a horizontal grid slice
- covered by the PR data swath: total, and within a 100 km radius of the GR site
- indicating Rain Certain: total, and within 100 km
- indicating convective rain type: total, and within 100 km
- indicating stratiform rain type: total, and within 100 km
- indicating rain type "other": total, and within 100 km
- indicating No Rain: total, and within 100 km
- indicating bright band exists: total, and within 100 km.

The time and distance of the nearest approach of the TRMM orbit track to the ground radar site and the start time of the GR volume scan are also stored in the database. Queries to the database allow an analyst to easily identify events with significant areal precipitation, precipitation of a given type (convective or stratiform, or unknown), or precipitation events where the orbital track is within a threshold distance of the ground radar. All associated PR and GR data files are cataloged in the database and linked to the site overpass events, making it easy to assemble the data files for significant events. As most site overpass events have no precipitation echoes, the preprocessed metadata in the database permit identification of rainy overpass events without the need to process all the data or make complicated time/space associations to external data sources.

On average, about 48 coincident events with available matching PR and GR data are collected each month for each of the WSR-88D ground radars listed in Table 1. Due to their proximity to the top of the TRMM orbit, the northernmost sites in the table experience about twice the number of coincident overpasses as the southernmost sites.

PR-to-GR match-up products are generated only when an overpass event occurs during a "significant precipitation event," as indicated in the stored metadata for the event. A significant precipitation event is defined as one in which at least 100 grid points within 100 km of the radar indicate Rain Certain (as defined in the PR product 2A-25). In the period from 8 August 2006 through 25 March 2009, a total of 32,244 coincident overpass events at the WSR-88D sites were recorded by the VN. Of these, 2,478 events met the significant precipitation criteria, and 2,292 of these had matching GR data available. Thus, per site and per month, about four coincidence events meet the criteria for a VN rainfall event, with about 3.5 per month of these having both PR and GR data.

2.1 *Improved VN Volume Matching Algorithm*

For those site overpass events meeting the significant precipitation event criteria, the resampling component of the VN software suite performs a geometric match-up of the PR and GR data. An earlier "legacy" version of the VN software (Morris, et al., 2007) involved resampling the data to a fixed 3-D Cartesian grid centered on the radar site. The legacy version and its results will not be further discussed in this paper.

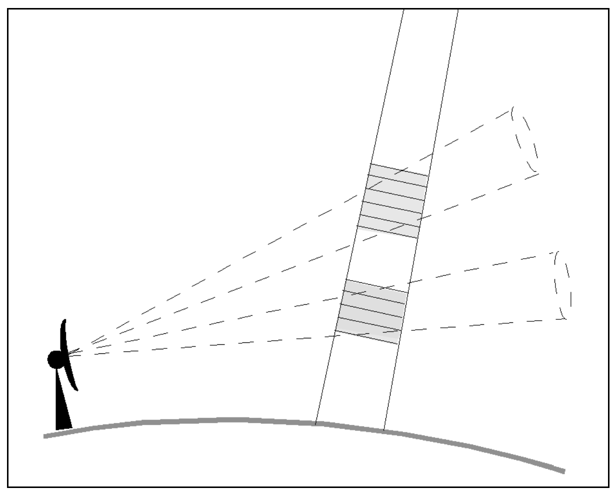

Figure 1. Schematic of PR gate averaging at GR sweep intersections. Shaded areas are PR gates intersecting two GR sweeps (dashed) at different elevation angles. Only one PR ray is shown. PR gates are 250 m along-ray by ~5 km in the horizontal.

The current, improved algorithm to match PR and ground radar (GR) reflectivity data, described below, is based on calculating PR and GR averages at the geometric intersection of the PR rays with the individual GR radar elevation sweeps. The along-ray PR data are averaged only in the vertical, between the top and bottom height of each GR elevation sweep it intersects (Figure 1). The GR data are averaged only in the horizontal within the individual elevation sweep surfaces, over an approximately circular area centered on each intersecting PR ray's parallax-adjusted profile (Figure 2). Reflectivity is converted from dBZ to Z before averaging, then the average Z is converted back to dBZ. This technique thus averages the minimum number of PR and GR full-resolution space and ground radar bins needed to produce spatially-coincident sample volumes. The output of this technique is a set of vertical profiles for a given rainfall event, with coincident PR and GR samples located at essentially random heights along each individual profile. The advantages of the current technique over gridded approaches are that there is no interpolation, extrapolation, or oversampling of data, so matching volumes only exist at locations where both the PR and GR instruments have taken actual observations. Other than for the averaging required to produce the matching volumes, the data are not smoothed; and each sample volume carries a set of attributes that describe the precise spatial, temporal, and quality characteristics of the sample. By convention, the intersection points processed in the match-up are restricted to those where the intersection of the PR ray with the earth surface is within a 100 km radius of the GR site.

The basic PR data processing algorithm is as follows:

1. For each PR ray in the product, compute the range of the ray's earth intersection point from the ground radar location. If greater than 100 km (adjustable), ignore the ray. If within 100 km, proceed as follows:
2. Examine the corrected reflectivity values along the PR ray. If one or more gates are at or above a specified threshold (18 dBZ), proceed with processing the ray, otherwise set the PR and GR match-up values to "below threshold".
3. Using the range from step 1, determine the height (assuming standard refraction) above ground level where the PR ray intersects the centerline of each of the elevation sweeps of the GR, and the vertical width of the GR beam at this range;
4. Compute a parallax-adjusted location of the PR footprint center at each GR sweep intersection height from step 3, as a function of height, the PR ray angle relative to nadir, and the orientation (azimuth) of the PR scan line. Retain these adjusted horizontal locations for the processing of the GR data;
5. Using the beam heights and widths from step 3, compute the upper and lower bound heights of each GR sweep at its intersection with the PR ray;
6. For each GR sweep intersection, determine the total number, and along-ray positions, of the PR range gates located between the upper and lower bound heights from step 5;
7. For the PR 3-D fields, perform a simple average of values over the set of range gates identified in step 6, for each GR sweep intersection (Figure 1). Reflectivity is converted from dBZ to Z before averaging, then the average Z is converted back to dBZ. Only those gates with values at or above specified reflectivity (18 dBZ) or rain rate (0.01 mm h^{-1}) thresholds are included in the average. Keep track of the number of below-threshold PR gates rejected from the vertical averages, and the number of gates expected in the averages from a geometric standpoint (from step 6);
8. For the 2-D PR field values (e.g., surface rain rate, bright band height), simply extract or derive the scalar field value for the given PR ray.

The 3-D PR fields which are vertically averaged, yielding one value per intersected GR sweep per PR ray, include:

- Raw PR reflectivity (Zr, in dBZ) from TRMM product 1C-21
- Attenuation-Corrected PR reflectivity (Zc, in dBZ) from TRMM product 2A-25
- Rain rate (mm h^{-1}) from TRMM product 2A-25
- Combined PR/TMI (TRMM Microwave Imager) rain rate from TRMM product 2B-31.

The 2-D PR variables which are taken unaveraged, one value per PR ray, include:

- Surface type (land/ocean/coastal) flag
- Near-surface rain rate, mm h^{-1}
- Bright band height
- Rain type categorization (convective, stratiform, other)
- Rain/no-rain flag.

These scalar values are directly extracted and/or derived from data fields within PR products 1C-21 and 2A-25.

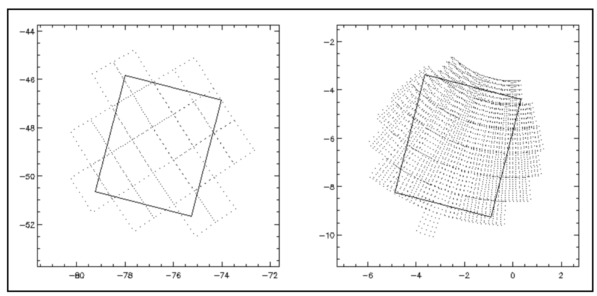

Figure 2. Schematic of ground radar bins (dotted) horizontally averaged over a near-circular area centered on a PR footprint (solid) plotted as a rectangular area, at far (left) and near (right) ranges from the GR. Axes show x- and y-distance from GR, in km.

The basic GR data processing algorithm is as follows:

1. For each PR ray processed, and for each elevation sweep of the GR, repeat the following:
2. Compute the along-ground distance between each GR bin center and the parallax-adjusted PR footprint center (from PR step 4);
3. Flag the GR bins within a fixed distance of the PR center. The fixed distance is equivalent to the maximum radial size of all the PR footprints processed (approximately 5 km).
4. Examine the reflectivity values of the flagged GR bins from step 3. If all values fall below a 15 dBZ threshold, then skip processing for the point and set its match-up value to "below threshold". Otherwise:
5. Perform an inverse distance weighted average of the GR reflectivity values over the bins from step 4 (Figure 2), using a Barnes gaussian weighting.

Reflectivity is converted from dBZ to Z before averaging, then the average Z is converted back to dBZ. All GR bins with values at or above 0.0 dBZ are included in the average. Keep track of the total number of bins included in the average, and the number of these bins with values below the specified GR reflectivity threshold (15 dBZ).

In summary, the PR data resolution is reduced in the vertical to the resolution of the GR, which varies with range from the ground radar, and varies in vertical coverage by the number of elevation sweeps of the ground radar. The GR data is reduced to the PR's horizontal resolution in PR (scan,ray) coordinates.

The input GR product consists of quality-controlled reflectivity data in a Universal Format (UF) data file (Barnes, 1980), or a TRMM GV 1C-51 HDF file, or a legacy-format WSR-88D Level-II Archive data file (i.e., pre-super-resolution), each of which contains data for a single, complete volume scan.

VN output products are in the form of binary netCDF files containing the volume-matched PR and GR data. Each VN netCDF data file corresponds to a single site overpass event, and contains all the PR and GR volume match data for the event. The basic structure of the VN netCDF match-up files is the same for all events. However, the dimensions of the data contained in the files vary, depending on the number of PR footprints that fall within a 100 km radius of the GR site for a given overpass event, and the number of unique elevation sweeps contained in the GR volume scan. In addition, the vertical and horizontal locations of the data points are unique for each event, and for each point within the event, as they depend on the juxtaposition of the (essentially random) TRMM orbital subtrack and the fixed GR locations, and on the GV volume scan strategy (elevation angles of the sweeps).

In essence, the volume-matched data are structured as a series of conical data layers, one layer for each unique elevation angle of the ground radar volume scan. Rather than being in the usual range/azimuth polar coordinates of the GR, the horizontal location and resolution of the data in the layer are defined by the scan/ray coordinates of the cross-track scanning PR, while the vertical bounds of each volume are defined by the top and bottom the GR elevation sweep at the location where the PR ray intersects the GR sweep. The data lend themselves to a Plan Position Indicator (PPI) display representation. Figure 3 shows an example of PR and GR volume-matched data plotted in PPI format, with range rings at 50 and 100 km range. Note that the data cut off at 100 km range and/or at the edge of the PR scans. PR volume-match data are normally missing at small ranges from the GR due to the low scan height above the surface, where PR bins near the surface are blanked out by the PR surface clutter algorithm.

In generating volume average reflectivity and rain rate values for each match-up volume, the VN algorithm calculates: (a) the number of PR and GR gates *expected* to be included in the averages from a strictly geometric standpoint, and (b) the number of these PR and GR gates falling below the applicable measurement threshold and *rejected* from inclusion in the averages. These metrics are stored in variables in the match-up netCDF file, and can be used to assess the "goodness" of the match-up between the radars. In statistical analyses of the data, effects of non-uniform beam filling and biases related to the detection threshold of the PR may be minimized by limiting the data points to those where the percent of rejected gates is at or near zero for both the GR and PR volume averages. Figure 4 shows the effect of filtering matchup data to points where fewer than 5% of the PR and GR gates were rejected by their

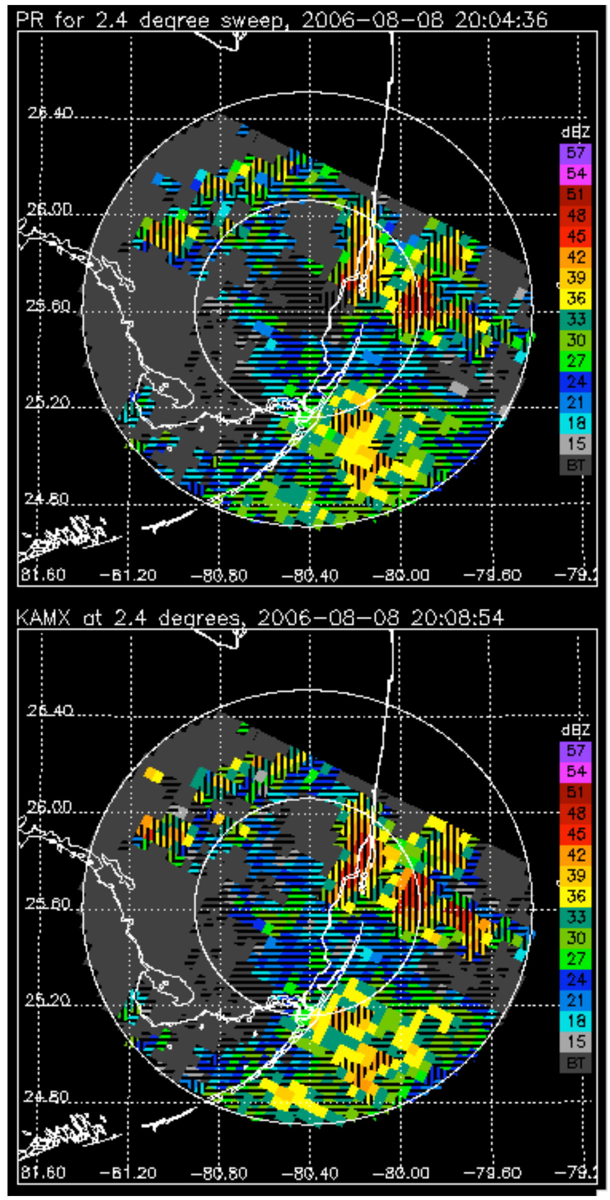

Figure 3. PR (top) and GR (bottom) volume-matched data for the KAMX (Miami, FL) PR overpass at 2004 UTC on 8 August 2006, on the 2.4° elevation sweep, plotted as PPIs. Vertical (horizontal) [no] hatching indicates convective (stratiform) [unknown] rain type.

respective reflectivity thresholds. Only the PR data are shown in Fig. 4.

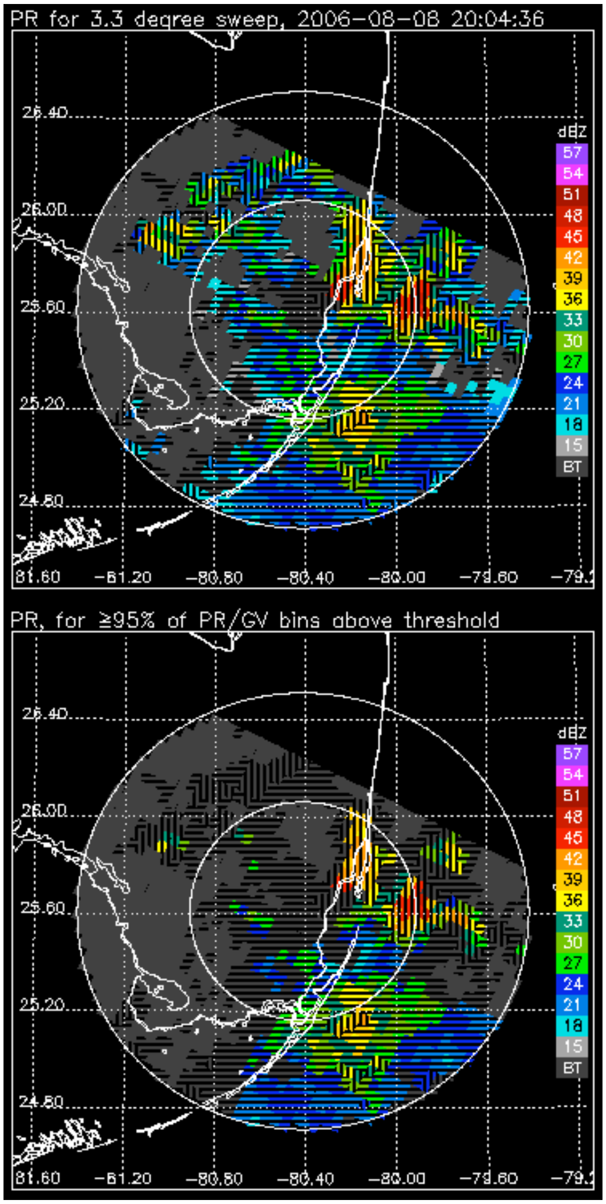

Figure 4. Total (top) and filtered (bottom) PR volume-matched data for the case in Fig. 3, but at 3.3° elevation. Data where 5% or more of the PR or GR gates in the volume averages were below reflectivity thresholds are grayed-out in the lower PPI.

3. STATISTICAL COMPARISONS

Site-specific PR-GR reflectivity comparison statistics have been generated from the match-up data. The statistical products provide information on the reflectivity calibration accuracy and stability of the WSR-88D radars relative to the PR. In this analysis 2363 overpass events with significant rainfall were evaluated. The data were collected during the period from August 8, 2006 through March 22, 2009. All results to follow use the attenuation-corrected PR reflectivity from the TRMM 2A-25 product. The data are stratified into convective and stratiform sample points, based on the Rain Type flag derived from the TRMM 2A-23 product. Radar frequency corrections defined by Liao and Meneghini (2009) were applied to the GR data to account for the differences in reflectivity factor that occur when the same rain or snow targets are observed by S- and Ku-band radars. The snow correction was applied to data above the bright band, and the rain correction was applied to the data samples below the bright band.

The stratiform points above the bright band, where PR attenuation is minimal, and where convective reflectivity gradients and bright band effects are not a factor, are the echo areas where the best agreement is expected between the PR and the GR radar. In our study, the assumptions are that the PR is stable and well calibrated, and the mean differences between the PR and GR for the stratiform/above bright band case are primarily due to GR calibration offsets. Table 2 presents the PR-GR bias (computed as the mean difference in dBZ) for individual ground radars, for both the frequency-corrected GR reflectivity (GR) and the original S-band GR reflectivity (GR_{Ku}). This dataset contains all samples categorized as stratiform rain type, with bottoms 500 m or more above the bright band, and where fewer than five percent of PR and GR bins were rejected as "below threshold" in the sample averages. Events where fewer than five sample points meet the criteria are excluded from the results. Each volume match sample is weighted equally in the calculations.

Radar ID	$PR\text{-}GR_{Ku}$ Mean Difference (dBZ)	PR-GR Mean Difference (dBZ)	PR Mean Reflectivity (dBZ)	Total Samples
KAMX	0.03	-0.49	22.65	2304
KBMX	-0.77	-1.47	23.90	12194
KBRO	-0.51	-1.12	23.15	2009
KBYX	0.04	-0.49	22.77	1042
KCLX	-0.76	-1.42	23.54	9071
KCRP	0.51	-0.03	23.37	2808
KDGX	0.07	-0.53	23.65	7266
KEVX	-0.07	-0.68	23.61	6488
KFWS	0.97	0.43	23.78	11910
KGRK	2.63	2.19	24.19	6871
KHGX	-0.09	-0.68	23.46	3332
KHTX	0.44	-0.16	23.96	12141
KJAX	-0.72	-1.33	22.95	4509
KJGX	0.73	0.17	23.81	6569
KLCH	-1.34	-2.06	23.54	4071
KLIX	-1.46	-2.15	23.18	7955
KMLB	0.71	0.26	22.52	2787
KMOB	1.00	0.50	23.37	4772
KSHV	-1.04	-1.71	23.35	8000
KTBW	-0.98	-1.62	22.99	3309
KTLH	-1.62	-2.34	23.37	3280

Table 2. Mean reflectivity difference (dBZ) between PR and original (GR) and frequency-corrected (GR_{Ku}) WSR-88D for stratiform rain volumes above the bright band. Negative values indicate WSR-88D higher than TRMM PR.

The frequency-corrected biases for most radar sites in Table 2 are less than 1 dBZ, with a few notable exceptions. KGRK (Fort Hood, Texas) shows a positive PR-GR bias, indicating a negative calibration offset in the KGRK radar relative to other WSR-88D sites when the data for the full time period are aggregated (more about this site below). Several adjacent WSR-88D sites near or along the Gulf coast between Louisiana and Florida (KLCH, KLIX, KSHV, KTBW, KTLH) exhibit a PR-GR bias of -1 dBZ or lower, indicating a high calibration offset of the WSR-88D radars relative to the PR. This set of Gulf coast radars, KEVX and KMOB excepted, seem to be well calibrated to one another, but run “hot” compared to the other WSR-88D sites in the VN subset.

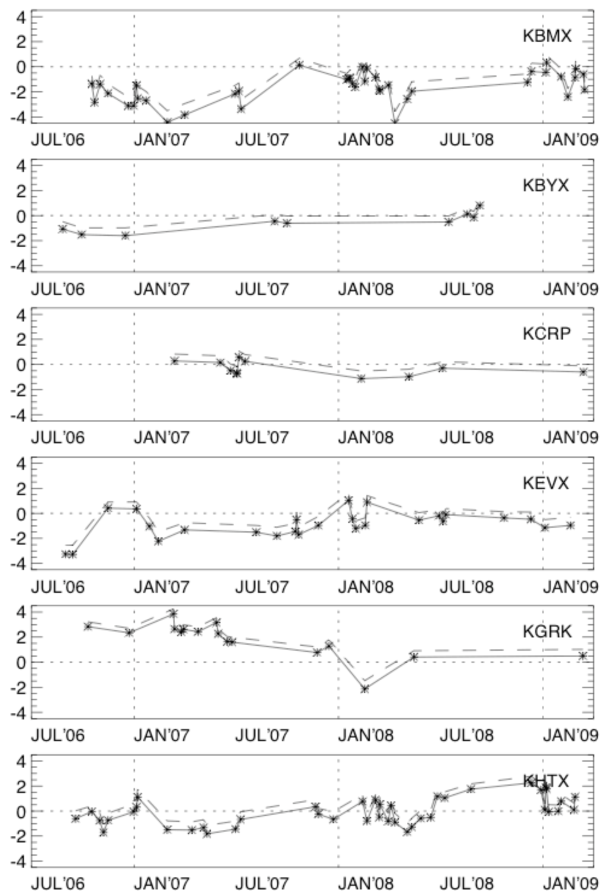

Figure 5. Time series of PR-GR mean reflectivity difference (dBZ) for stratiform precipitation above the melting layer, for six WSR-88D sites in the VN. Solid (dashed) lines plot differences using original (frequency adjusted) GR data.

The stability of the WSR-88D calibrations has been investigated by generating time series of PR-GR mean reflectivity difference. Figure 5 shows the time series for a subset of the WSR-88D sites in the VN, where each point plots the mean reflectivity difference for a site overpass event with active precipitation echoes. Figure 5 uses the same criteria as in Table 2 (stratiform rain, above bright band, having five percent or fewer bins below threshold in sample averages), with the additional constraint that, to reduce noise, at least 25 sample points must meet the criteria for the event to be included in the plot. While KGRK shows a negative GR bias with respect to the PR over the full dataset (Table 2), Fig. 5 shows that the events with consistently negative biases occur prior to mid-2007, and KGRK had improved to near-zero mean bias after mid-2007. KBYX and KCRP exhibit both low reflectivity bias and stable calibration relative to the PR, but had fewer rainy overpass events overall.

Outlier events in the time series plots often correspond to marginal precipitation events. The number of points in each event that meet the stated criteria can vary by over two orders of magnitude. PR-GR mean reflectivity differences by event tend towards lower biases as the area of precipitation becomes more widespread, but for most sites, an insufficient number of such events exists to be represented as a meaningful time series.

4. ANALYSIS AND VISUALIZATION TOOLS

A suite of visualization tools, written in Interactive Data Language (IDL; www.ittvis.com), has been developed for viewing and analyzing the VN geometry match-up data sets for individual site overpass events. The two primary tools are the statistical analysis tool and the vertical cross section tool. For orientation purposes, the statistical analysis tool displays user-selected PPIs as shown in Fig. 3 in the form of an animation loop progressing from low to high elevation sweeps. For the statistical computations themselves, the statistical analysis tool stratifies the event data into vertical layers in two manners: (1) by height above the surface, in 1.5-km-deep layers, for 15 levels centered from 1.5 to 19.5 km, and (2) into three layers defined by proximity to the bright band (melting layer): above, within, and below. The statistical analysis tool uses the vertically-stratified data to produce a number of tabular and graphical displays, including vertical profiles of PR and GR reflectivity from match-up data averaged over the constant height levels; histograms of PR and GR reflectivity for match-up data stratified by proximity to the bright band (below, within, and above); scatter plots of PR vs. GR reflectivity categorized by rain type (convective or stratiform) and proximity to the bright band; and tables of PR-GR mean difference broken out by rain type, for both the constant-height data levels and the levels defined as proximity to the bright band. The statistical analysis tool supports studies of calibration differences between the PR and GR as well as the evaluation of the quality of the TRMM PR attenuation correction algorithm.

The vertical cross-section tool generates cross sections of the PR and GR reflectivity match-up data and PR-GR reflectivity difference along a selected PR scan line (perpendicular to the TRMM orbit track). If the original 2A-25 TRMM PR product files are available, cross sections of full-vertical-resolution (250 m) PR data can also be displayed for comparison to the volume-averaged PR match-up data. The cross-section tool was developed primarily to investigate differences seen between the PR and GR volume match data within and below the melting layer in stratiform rain, and to evaluate the quality of the PR attenuation correction algorithm in convective and heavy stratiform rain cases.

Both tools provide the ability to apply the Liao/Meneghini S-band to Ku-band frequency adjustments to the reflectivity data, and to filter the data volumes according to the percent above threshold criteria described in Section 2.1. These software tools are being made available online as open source code via the NASA/GSFC Innovative Partnerships Program Office (http://opensource.gsfc.nasa.gov). User manuals for each tool include examples of each of the graphics and tabular summaries described in this section, and the interested reader is referred to these documents to view the example products and for a full description of the tool display and analysis capabilities. The user manuals are available packaged with the open source code, or from the GPM GV web site referenced in the next section.

5. CONCLUSIONS

The VN prototype has provided data, procedures, and software tools needed to evaluate the current TRMM PR attenuation correction algorithm as well as the stability and accuracy of the WSR-88D calibration at individual sites in the radar network. Improvements to the PR-to-GR volume matching algorithm have boosted the confidence in the quality of the comparison of the observations taken by the two types of radars, and new data visualization tools provide flexibility to the analyst in the manner in which the data are analyzed and displayed.

The PR-to-GR reflectivity comparisons show generally good agreement between the PR and WSR-88D in the stratiform/above melting layer category, with mean differences at most sites within 1 dBZ. Several adjacent WSR-88D sites along the Gulf Coast show a high calibration bias relative to the PR, but are closely calibrated to one other. Only one WSR-88D site (KGRK – Fort Hood, Texas) shows an obvious and significant change in calibration over the analyzed time period.

It is expected that the procedures developed for the VN prototype will be used operationally for validating the attenuation correction and precipitation retrieval algorithms of the Dual-frequency Precipitation Radar (DPR) in the GPM era. In the near term, the site-specific calibration differences seen in the WSR-88D data may assist the National Weather Service (NWS) to improve the reflectivity calibration and quantitative precipitation estimates from these radars. The VN prototype will also be applied to the evaluation of TRMM PR Version 7 products currently under development.

The VN routinely ingests and processes PR subset products and matching GR data for 21 WSR-88D sites. The VN prototype has been designed to be scalable, and can readily be configured to add more U.S. domestic and international validation sites. Additional participants are welcome to add data for their GR sites to the network. Information about the match-up data files and statistical products, including documentation and how to gain online access to them, can be found on the GPM ground validation web site located at this URL: http://gpm.gsfc.nasa.gov/groundvalidation.html.

6. ACKNOWLEDGEMENTS

The authors would like to thank the TRMM Ground Validation Office for acquiring and preprocessing the WSR-88D data used in the VN, and for hosting the ftp site for the VN data. In particular, the ongoing efforts by Jason Pippitt of TRMM GV to perform the manual quality control and review of the WSR-88D data are acknowledged.

7. REFERENCES

Anagnostou, E.N., C.A. Morales, and T. Dinku, 2000: The use of TRMM Precipitation Radar observations in determining ground radar calibration biases. *J. Atmos. Ocean. Tech.*, **18**, 616-628.

Barnes, S. L. (1980): Report on a meeting to establish a common Doppler radar data exchange format. *Bull. Amer. Meteor. Soc.*, Vol. 61, No. 11, 1401-1404

Bolen, S.M. and V. Chandrasekar, 2000: Quantitative cross validation of space-based and ground-based radar observations. *J. Appl. Meteor.,* **39**, 2071-2079.

Keenan, T., K. Glasson, F. Cummings, T.S. Bird, J. Keeler and J. Lutz, 1998: The BMRC/NCAR C-Band Polarimetric (C-POL) Radar System. *J. Atmos. and Oceanic Tech*., **15**, 871-886.

Liao, L., R. Meneghini, and T. Iguichi, 2001: Comparisons of rain rate and reflectivity factor derived from the TRMM Precipitation Radar and the WSR-88D over the Melbourne, Florida, site. *J. Atmos. Ocean. Tech*., **18**, 1959-1974.

Liao, L., R. Meneghini, 2009: Changes in the TRMM Version-5 and Version-6 Precipitation Radar Products due to Orbit Boost. *J. Meteor. Soc. Japan*. (Submitted)

Morris, K.R, M.R. Schwaller, D.B. Wolff, and J.L. Pippitt, 2007: A Global Precipitation Mission (GPM) validation network prototype. *Preprints*, 34th Conference on Radar Meteorology of the AMS, Cairns, Australia, 5-10 August 2007.

Schumacher, C., and R. A. Houze, Jr., 2000: Comparison of radar data from TRMM satellite and Kwajalein oceanic validation site. *J. Appl. Meteor*., **39**, 2151-2164.

Wolff, D. B., D. A. Marks, E. Amitai, D. S. Silberstein, B. L. Fisher, A. Tokay, J. Wang, and J. L. Pippitt, 2005: Ground validation for the Tropical Rainfall Measuring Mission. *J. Atmos. Ocean. Tech*, **22**, No. 4, 365-380.